12

Optimization of mass separators

© V.V. Lukashevich

St. Petersburg Nuclear Physics Institute, National Research Center Kurchatov Institute,
188300 Gatchina, Russia
e-mail: lukashevich_vv@pnpi.nrcki.ru

Received March 23, 2021
Revised June 14, 2021
Accepted June 16, 2021

The optimization of separator masses in this paper is based on the realization of the linearity of the system under study and the consequences of Liouville's theorem. The properties of several mass separators with an ion energy of 30 keV and a beam emittance of 4 mm · mrad are considered. Focusing is provided by an aberration-free lens and a magnetic corrector. Phase diagrams along the beam path are in the form of parallelograms, which indicates the absence of geometric aberrations. For each of the separators, the resolution calculated in the linear approximation coincides with the simulation results. It is shown that a mass separator based on a magnet with a rotation angle of 54.7° has a resolution of about 5000, and a separator based on two magnets with a rotation angle of 45° and 90°, respectively, has a resolution of 14 000–15 000.

Keywords: ion optics, emittance, lenses, phase diagram, aberrations.

DOI: 10.21883/TP.2022.14.55230.76-21

Introduction

Since the appearance (1967) of the first ISOLDE (isotope separation on line device) system at CERN, -separators have appeared in many laboratories around the world. Although the properties of these installations as a whole and the properties of their constituent focusing elements are well studied, the available mass-separators do not have high resolution. The declared high resolution of separators at the stage of their calculation and design with hardware implementation turned out to be several times less than the calculated ones. The reason is that the optical elements of the ion beams forming at the entrance to the analyzing magnet have significant aberrations that cannot be controlled by the available diagnostic tools and which are not eliminated when using multipole correctors. For most separators, the value of the ion beam emittance is unknown, and the type of phase diagrams along the beam path is also unknown.

In this paper, when optimizing the parameters of the masses of -separators, two statements are implemented. Firstly, the optical system, to which the mass-separators can be attributed, can be of high quality only if this system is linear. Secondly, according to Liouville's fundamental theorem on the conservation of phase volume, with a constant ion beam emittance, the beam width is smaller the greater is the angular spread of particle trajectories. In the terms of separators, this means that in order to increase the resolution of the beam at the entrance to the magnet, one should strive to make it as wide as possible. At the same time, since the sector magnet is a focusing element, the angles of inclination of the trajectories will increase at the exit of the magnet and, accordingly, the beam width in the focal plane will decrease, i.e., the resolution will increase.

The optimal mass characteristics of the -separator are achieved by means of computer modelling, which consists in calculating the distribution of electrostatic fields between the electrodes of the lens system and the magnetic field of the magnet, solving the equation of motion, which makes it possible to determine the parameters of the trajectories of particles in the ion beam in any beam section. These parameters are presented in the form of phase diagrams, which make it possible to evaluate the quality of focusing and optimize the focusing system. The task is to achieve the linearity of the transformation of the trajectory parameters. A similar procedure is described in the articles [1,2] and this study is their continuation. In the study [1] the technique of phase diagrams is developed, on the basis of which an aberration-free lens and electrostatic correctors of lens aberrations and dipole magnets are developed in [2].

The measurement of phase diagrams by simulation is the only possible way to diagnose a particle beam due to the impossibility of instrumental measurement of phase diagrams in the area of electromagnetic fields. Measurements of phase diagrams in fields-free regions of space, for example, in the focal plane of a magnet, do not allow us to judge the place of occurrence of aberrations, their magnitude and nature.

1. Ion source

Let's define the parameters of the ion source and the beam emittance so that the mass-separator with an axially symmetric lens with an aperture of 100 mm and a rotation angle of 54.7° has a typical resolution of the order of 1000. This separator is used to calibrate the ion source.

The ion source of surface ionization in on-line mass-separators is a tube, one end of which is connected to the target, and at the edge of the other tube end there

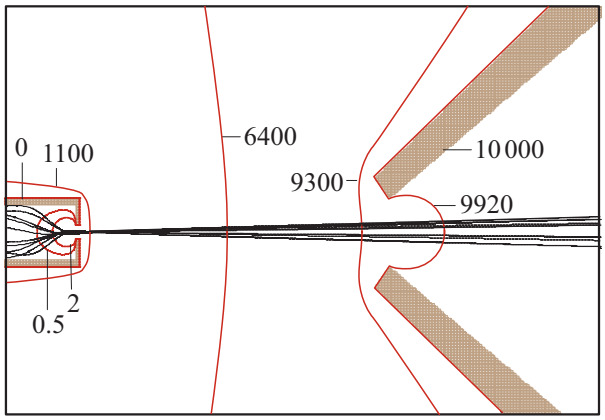

Figure 1. Ion source and extracting electrode. Several equipotential lines with ionic-optical potentials in volts are presented.

is a small hole for the exit of ions. The ions are pulled out and accelerated by an electric field arising from - due to the potential difference between the source and the pulling electrode. The magnitude of the ion current depends on this voltage and the current heating the tube. With an increase in the pulling voltage, the electric field penetrates deeper into the source, increasing the ion capture area, and an increase in the temperature of the tube increases the ionization efficiency.

From the experience of operating mass-separators, it is known that in the range of ion currents of picoamperes-nanoamperes, the shape of the mass line in the focal plane of the separator does not change. This indicates that the potential distribution created by the pulling electrode inside the source is not distorted by the volume charge of ions and the emittance of the beam is constant.

This paper describes a simple model in which a simulation program describes the generation of ions inside a source tube with an average energy of 0.1 eV, which corresponds to a temperature of 2000°K. Further, the equation of ion motion in the electric field found by solving the Laplace equation is solved.

Figure 1 shows the simulated ion source. The end hole has a diameter of 1 mm, and the inner diameter of the tube is 4 mm. The distance between the source and the pulling electrode is 20 mm. Inside the tube, ions are born with random trajectory slopes within a cone with an angular solution of 40° and are pulled out by an electric field created by a pulling electrode with a potential of 10 keV. At a distance of 0.8 mm from the end of the source there is a beam crossover. The electrostatic potential at this point is 1.58 kV.

The phase diagram of the beam at the crossover point at the outlet of the source is shown in Figure 2. The boundaries of the phase diagram are linear, which, according to the results of [1], indicates the absence of aberrations. Beam emittance η is equal to 16 mm · murad and when the ions accelerate to an energy of 30 keV becomes equal to 4 mm · mrad.

The shape of the phase diagram depends on the initial conditions. At other values of the pulling potential and other apex angles of the cone, the phase diagram can take the form of a parallelogram.

The mass-separator with such a beam emittance has a resolution of the order of 1000. The nonlinear phase diagram of the beam in front of the magnet is shown in Figure 3, *a* diagrams in the focal plane of the magnet and the spectrum of two masses $A = 100$ and 100.2 of this separator are shown in Figure 4.

An ion beam with an energy of 30 keV and an emittance of 4 mm · mrad will be used to test the separators described below.

In the monograph [3], the question is discussed, what will happen to geometric aberrations when the size of the optical element decreases? Will they tend to zero or to a finite limit? Opinions on this matter are divided, although there is no evidence of this or that claim.

It is possible to point to an equivalent device in the center of which the beam has the same phase diagram as in Figure 2. This device is a tube filled with particle trajectories. Trajectories with zero slopes are distributed

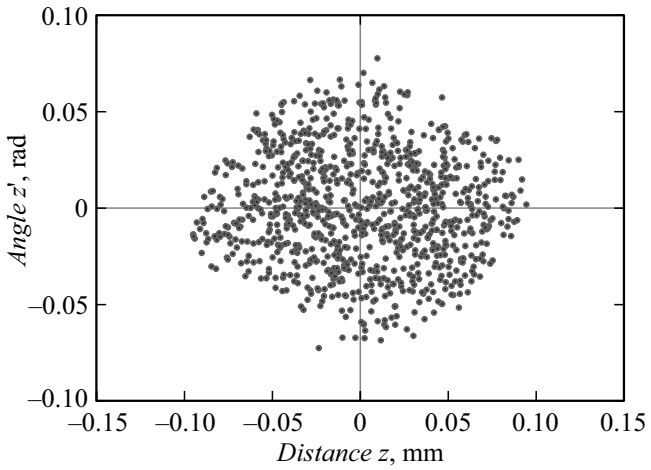

Figure 2. Phase diagram of a beam near an ion source.

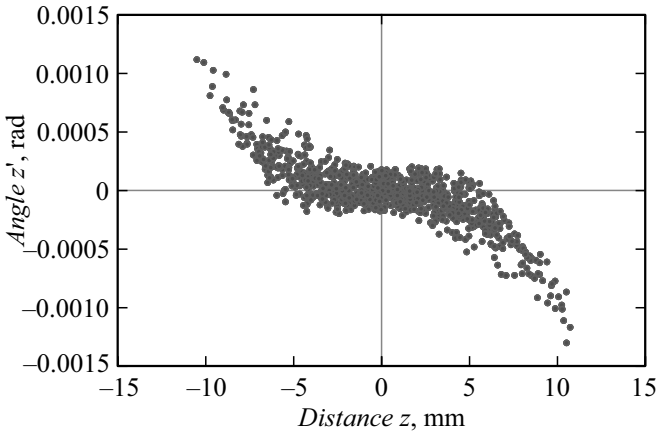

Figure 3. Phase diagram of the ion beam in front of the magnet.

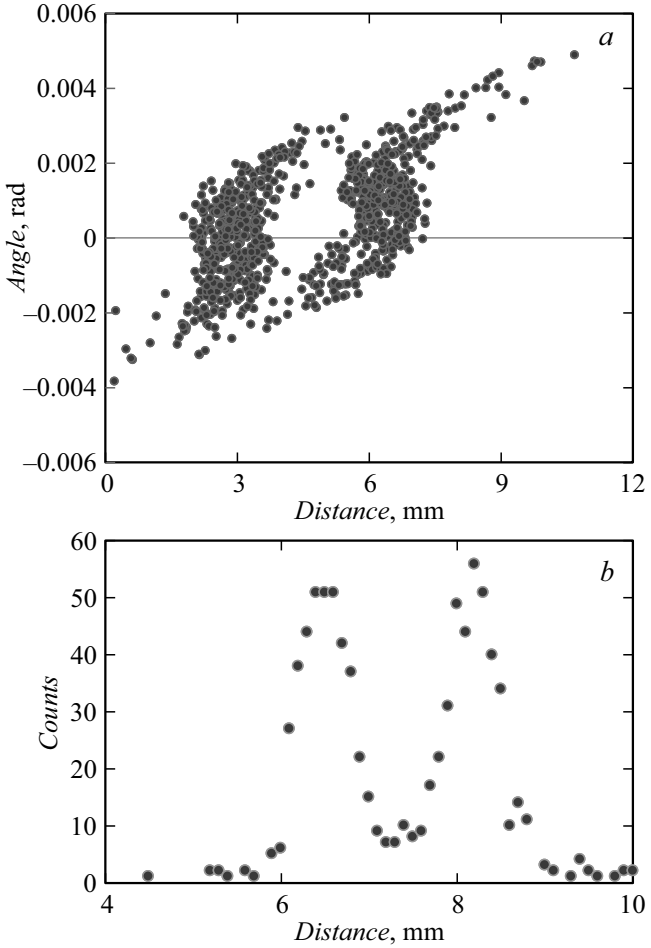

Figure 4. *a* — phase diagrams; *b* — mass spectrum 100 and 100.2.

over the diameter of the tube d and this diameter is equal to the interval 0.2 mm in Figure 2. It follows from the same figure that the trajectories in the center of the tube have maximum slopes equal to $z' = d/l = 0.08$ rad. Hence the length of the tube l is $0.2/0.08 = 2.5$ mm. A tube with a diameter of 0.2mm and a length of 2.5mm is a miniature device. Such an analogy indicates that the optics of an ion source can be considered as the optics of a small device and that such a device has no aberrations. This is not proof, but an indirect argument in favor of the fact that when the size of the electrostatic optics decreases, the aberrations are significantly weakened and, possibly, completely disappear.

2. Classification of magnets of masses of -separators

In the linear approximation, the equations of motion of particles in a magnetic field in the horizontal and vertical planes are separated and become independent. Solutions of these equations for trajectories can be presented in matrix form. These matrices have been known since 1953 g. [4], but since they are almost not found explicitly in the modern literature on ion optics, we will give them again. These are expressions (1) and (2 a).

$$M_z = \begin{pmatrix} \frac{\cos(\vartheta-\varepsilon_1)}{\cos\varepsilon_1} & \rho\sin\vartheta & \rho(1-\cos\vartheta)/2 \\ -\frac{\sin\Omega}{\rho\cos\varepsilon_1\cos\varepsilon_2} & \frac{\cos(\vartheta-\varepsilon_2)}{\cos\varepsilon_2} & \left(\sin\vartheta+\mathrm{tg}\,\varepsilon_2\times\right. \\ & & \left.\times(1-\cos\vartheta)\right)/2 \\ 0 & 0 & 1 \end{pmatrix}, \quad (1)$$

$$M_y = \begin{pmatrix} 1-\vartheta\,\mathrm{tg}\,\varepsilon_1 & \rho\vartheta \\ -\frac{1}{\rho}\left(\mathrm{tg}\,\varepsilon_1 - \mathrm{tg}\,\varepsilon_2(1-\vartheta\,\mathrm{tg}\,\varepsilon_1)\right) & 1-\vartheta\,\mathrm{tg}\,\varepsilon_2 \end{pmatrix}. \quad (2a)$$

The matrix (1) transforms the column

$$\begin{pmatrix} z \\ z' \\ \Delta m/m \end{pmatrix}, \quad (2b)$$

consisting of the deviation of the particle from the axis z, the angle of inclination z' and the relative mass spread. The column that transforms the matrix (2a) includes the magnitude of the deviation y and the angle of inclination y'.

In matrices (1), (2a) ρ — the radius of curvature of the trajectory, and the angle of rotation in the magnetic field $\vartheta = \Omega + \varepsilon_1 + \varepsilon_2$ consists of the angle of the sector Ω and the angle of entry of the particle beam into the magnet ε_1 and the angle of exit ε_2 accordingly.

With the help of these matrices, it is possible to design a magnet of the mass-separator, guided by the conditions of the physical problem, the available space for placing the installation and personal preferences.

In general, sector magnets can be classified by the type of ion beam at the entrance to the magnet, namely, the beam is approximately parallel and the beam diverges.

2.1. Sector magnet with input parallel beam

First, let us consider a magnet with a normally incident parallel input beam. The separator matrices in this case have the following form:

$$S_i = (l_i)(M_i), \quad (3)$$

where l_i is a matrix of field-free spaces between the output face of the magnet and its focal plane, and $i = z, y$ indicates the horizontal and vertical planes, respectively. These matrices have a simple form $(l_i) = \begin{pmatrix} 1 & l_i \\ 0 & 1 \end{pmatrix}$.

The matrix element $S_{i11} = 0$ gives equality for finding the lengths of free intervals l_z and l_y, and the magnet parameters are calculated from solving a system of two equations:

$$\Delta = l_z - l_y = 0 \quad \text{and} \quad d\Delta/d\varepsilon_2 = 0, \quad (4)$$

since in equality $\frac{d\Delta}{dm} = \frac{d\Delta}{d\vartheta}\frac{d\vartheta}{dm} = \frac{d\Delta}{d\varepsilon_2}\frac{d\varepsilon_2}{dm} = \frac{d\Delta}{d\varepsilon_2} = 0$ the derivative of the output angle by mass is the angular dispersion, which is nonzero.

The first in (4) equation is a double focusing condition, and the second — preservation of this condition in a wide range of masses.

The solution of the system (4) describes the well-known [5] magnet with parameters $\vartheta = 54.7°$, $\Omega = 19.2°$.

For a linearly focused particle beam, the phase diagram has the form of a parallelogram, the area of which (emittance η) is equal to the product of the length of the parallelogram, which we denote as $\overline{z}$, by the height representing the total angular spread $\overline{z}'$, $\eta = \overline{z}\overline{z}'$.

Let us substitute the width of the angular distribution $\overline{z}'$ in (2b) instead of the angle, then the matrix S_z transforms this value into the width of the particle deflection distribution equal to $S_{z12}\overline{z}'$. The mass spread also gives a z coordinate distribution equal to $S_{z13}\frac{\Delta m}{m}$. We equate these values and find the resolution

$$\tau = \frac{\Delta m}{m} = \frac{S_{z13}}{S_{z12}\overline{z}'} = \frac{S_{z13}}{S_{z12}}\frac{\overline{z}}{\eta} = 0.408\,\frac{\overline{z}}{\eta}, \qquad (5)$$

the numerical coefficient in this expression is obtained by substituting the angular parameters of the magnet into the matrix elements.

In expression (1) there are four angular parameters, and only three are independent. They can be chosen arbitrarily, for example, the angle of incidence ε_1, the angle of rotation of the particle ϑ and the angle of the sector is Ω. To find these parameters to a system of two equations (4) a third equation is added, which determines the maximum resolution depending on the angle ε_1. This equation has the following form:

$$\frac{d\tau}{d\varepsilon_1} = 0.$$

The parameters found in this way are $\varepsilon_1 = 18.6\ ^{circ}$, $\vartheta = 70°$ and $\Omega = 31.5°$ have a general purpose separator magnet (GPS) [6] in CERN. The resolution in this case is equal to

$$\tau = \frac{m}{\Delta m} = \frac{S_{13}}{S_{12}}\frac{\overline{z}}{\eta} = 0.571\,\frac{\overline{z}}{\eta}. \qquad (6)$$

From comparing this expression with the ratio (5), it follows that the gain in resolution is 1.4 times.

In cases where the geometry of space does not allow the separator to be installed on the basis of a single magnet, it may be possible to use the configuration of two magnets that rotate the particles in opposite directions. In this case, there is an intermediate focus between the magnets, after which the diverging beam falls on the second magnet.

2.2. Separator with input divergent beam

The source of ions in such a separator can be an intermediate focus or a slit on which the beam is focused. For simplicity, we assume that the beam is parallel in the vertical plane. This situation occurs when focusing a parallel beam with a sector magnet with a normal input and output.

Let us calculate the parameters of the second magnet in this case.

Using the expressions (1), (2a), for the separator matrices we can write the corresponding expressions for movement in the horizontal and vertical planes:

$$S_z = l_{z2}M_z l_{z1}, \qquad (7)$$

$$S_y = l_{y2}M_y. \qquad (8)$$

Here, the index 1 indicates the distance from the focus point of the beam (or slit) to the front face of the magnet, and the index 2 — indicates the output distance from the magnet to its focal plane. Since the width of the line should not depend on the angles of inclination of the trajectories of the diverging beam, the matrix element $S_{z12} = 0$. This is the condition of an optical image (or focusing from point to point), which in units of radius of curvature connects the values l_{z1} and l_{z2}:

$$l_{z1} = \frac{l_{z2}\cos\Omega/\cos\varepsilon_2 + \sin\vartheta}{l_{z2}\cos\Omega/\cos\varepsilon_2 - \cos\vartheta}.$$

Further, we minimize the size of the separator by putting, $\frac{dL}{dl_{z2}} = 0$, where L — the total length of the first and second intervals. As a result, a quadratic equation is obtained, the solution of which has the following form:

$$l_{z2} = \cos\varepsilon_2\,\frac{\cos\vartheta \pm 1}{\sin\Omega},$$

$$l_{z1} = \frac{\cos\Omega + \cos\varepsilon_2}{\sin\Omega}.$$

The angular parameters of the magnet are calculated in the same way as in the previous case, i.e. from the solution of a system of two equations. The first equation is a double focusing condition, and the second — is the same condition, but only for a wide range of masses. In an explicit form, this system has the following form:

$$\frac{1 + \cos(\Omega + \varepsilon_2)}{\sin\Omega} - \frac{1}{\sin\varepsilon_2} = 0,$$

$$\mathrm{tg}\,\Omega = \mathrm{tg}^3\,\varepsilon_2.$$

The solution is $\Omega = \varepsilon_2 = 45\ ^{circ}$, $\vartheta = 90°$, and for free intervals in units of radius of curvature, the following values are obtained: $l_{z1}/2 = l_{z2} = l_{y2} = \rho$, and the mass dispersion is 1.5ρ.

The resolution in the linear approximation, in which the phase diagram of the beam in the source is linear, is determined in this case as follows: $\tau = \frac{m}{\Delta m} = -\frac{S_{z13}}{S_{z11}\overline{z}} = \frac{S_{z13}\overline{z}'}{\eta} = \frac{1.5\rho\overline{z}'}{\eta}$, the matrix element 11 in this case is equal to one.

In this expression, the ratio of the emittance to the width of the slope angle distribution is equal to the width of the beam in the intermediate focus or the width of the input slit.

We note that separators of this type are not described in the world literature.

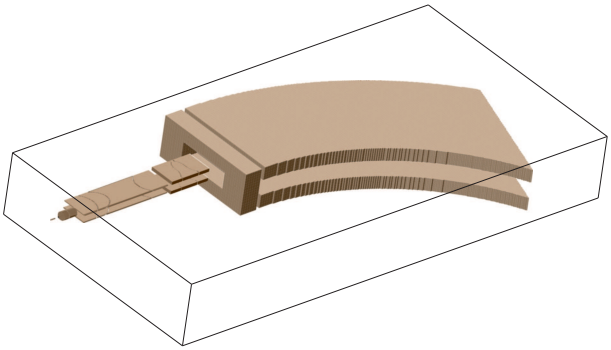

Figure 5. Mass-separator with ion source, aberration-free lens and magnet aberration corrector.

3. Optimization of the masses of separators

Let us consider the properties of a separator with a linear focusing system based on a sector magnet with a rotation angle $\vartheta = 54.7°$.

The device of the first optimized separator is shown in Figure 5. A short-circuited screen is installed in front of the poles of the magnet, which excludes the effect of the scattering field of the magnet on the course of trajectories in the focusing system. The formation of an ion beam is carried out using an aberration-free lens and a magnet aberration corrector, which are described in [2].

At each point of the beam path, the phase diagram is linear. Within the limits of the first, second and third electrodes of the lens, the beam diverges. Focusing occurs at the last field gap and after the fourth electrode, the beam becomes approximately parallel. The phase diagram of the beam at the ion outlet from the source is shown in Figure 2.

Figure 6 demonstrates the linear properties of the beam in the center of the second electrode.

The phase diagram at the lens outlet (Figure 7) at the end of the fourth electrode in front of the magnetic corrector characterizes a high degree of linearity of focusing. The maximum divergence angles of the trajectories are $\pm 5 \cdot 10^{-5}$ rad.

As described in [2], the linearity of focusing along the beam path was achieved using an iterative procedure consisting in selecting the geometric shape of the electrodes and the electrical potentials on them.

From each phase diagram, it is possible to obtain the profile of the particle beam and the distribution of particles at the angles of inclination of the trajectories. In the first case, the diagram is convoluted by angle, and in the second — convolution by distance to the axis. Such convolutions of the diagram shown in Figure 7 are presented in Figure 8.

Substituting into the expression (5) the total angular width of the beam from Figure 7 (0.12 mrad), we obtain the expected resolution of the separator at the level of 3000. If we use the angular width at half the height of the distribution of Figure 8, *b*, then the resolution will be equal to 4500. These numbers are comparable to the results obtained in the focal plane of the magnet during modelling.

A corrector with a potential of the average electrode 5 V corrects minor aberrations of the magnet, as a result of which the phase diagrams of the two masses $A = 100$ and 100.1 in the focal plane of the magnet have linear boundaries. These diagrams and their convolution by angle are shown in Figure 9. The resolution, determined by the width of the line at half the height of Figure 9, *b*, is equal to 4500–5000.

This resolution is up to 5 times higher than the resolution of separators of this type available in various laboratories around the world.

When the beam falls obliquely on the front face of the magnet, in accordance with the expression (6), the resolution will be 1.4 times higher.

Note that the obtained resolution is the limit for the described system and is due only to the spread of the phase parameters of the beam.

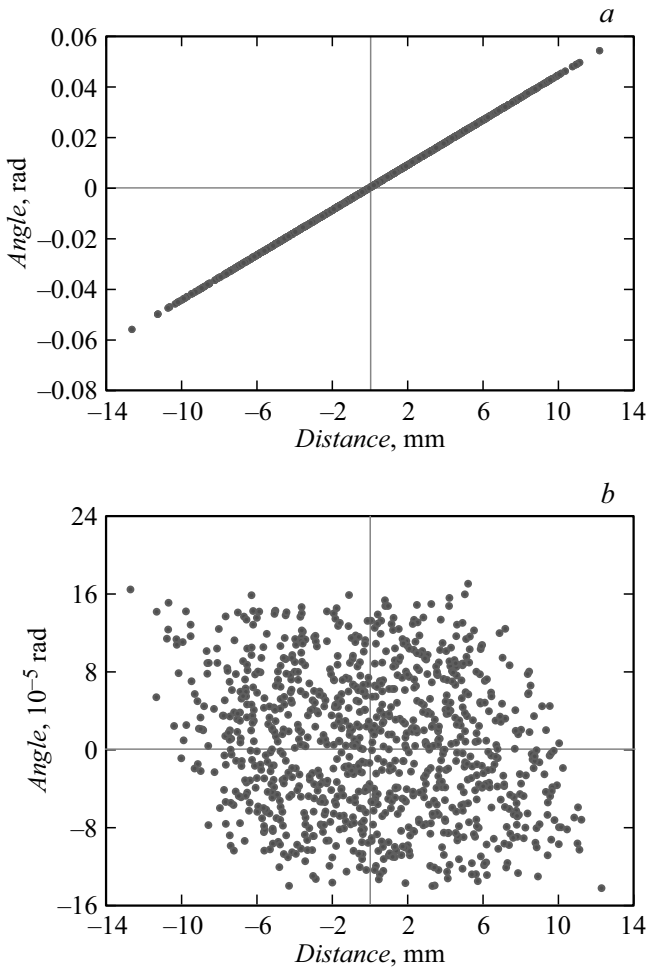

Figure 6. *a* — diagram of the divergent beam in the center of the second electrode of the lens; *b* — the same diagram after being brought to the form in the crossover.

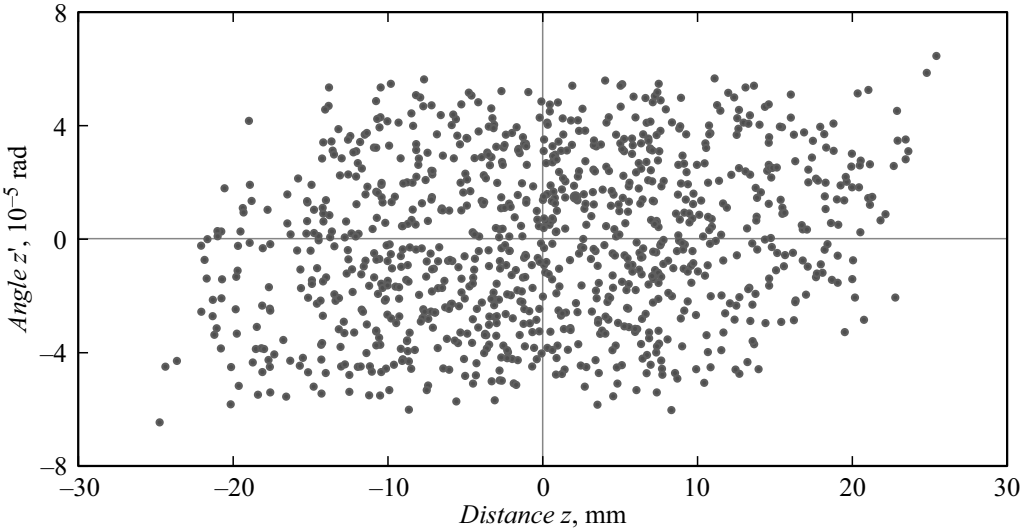

Figure 7. The phase diagram of the beam in front of the magnetic corrector.

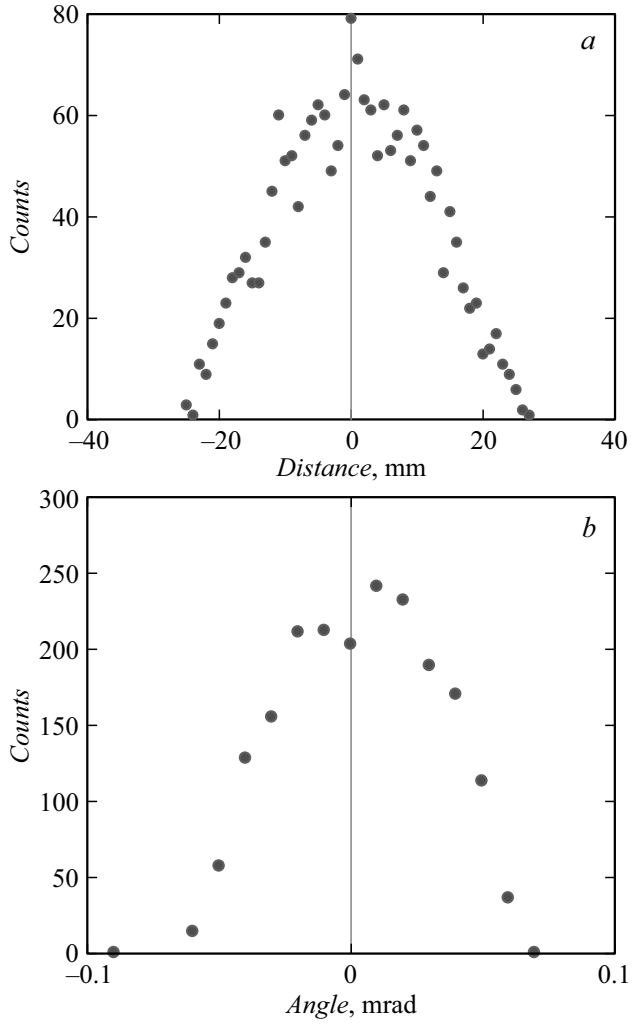

Figure 8. Convolution of the phase diagram Figure 7: *a* — by angle; *b* — by distance.

Modelling the effect of chromatic aberrations on the resolution of the separator leads to the conclusion that the instability of the accelerating voltage of the order of 10^{-5} and the energy spread in the ion source from 0.05 to 0.2 eV are not significant for the described separator. These aberrations make a big contribution only with a resolution of the order of 100,000 and above.

3.1. Separator based on two magnets

Consider the properties of a separator consisting of a sector magnet with a particle rotation angle of $\varphi = 45°$ and the magnet just described with a rotation of $\vartheta = 90°$. This combination of magnets makes it possible to place them on the neutron channel of the PIK reactor of the St. Petersburg Institute of Nuclear Physics without overlapping the experimental zones of neighboring channels.

The type of separator is shown in Figure 10. An ion source, a linearly focusing lens and a magnetic corrector are installed in front of the first magnet. The same corrector is located in front of the second magnet.

A separator with two magnets has a number of useful properties. Firstly -, the resolution increases, since the dispersions of the two magnets are summed up, and secondly, it is easier to organize neutron protection on the first magnet when installing a separator on the neutron channel of the reactor.

Separator matrices are obtained from matrices (7) after multiplying from the right by the product $l'_{z2}M_{45}$, where the multipliers are the matrices of the magnet and the free gap magnet-focal plane. For a given magnet, this gap is equal to the radius of curvature.

The resolution is determined by matrix elements having the following form:

$$S_{13} = \frac{\rho}{2}\left[2 - \cos\vartheta + \frac{\sin\vartheta(\cos\Omega + \cos\varepsilon_2)}{\sin\Omega}\right], \quad (9)$$

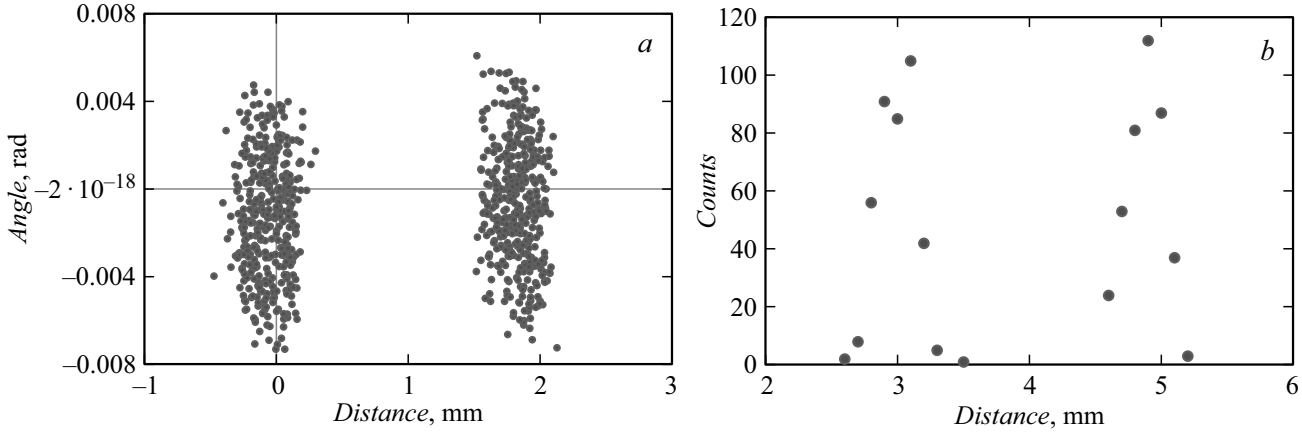

Figure 9. Phase diagrams (u) and mass lines (b) of an ion beam with masses 100 and 100.1.

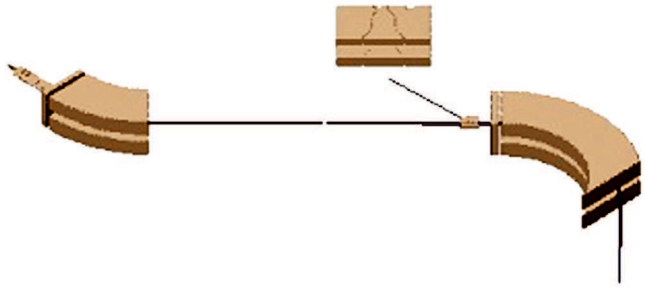

Figure 10. Separator based on two magnets. The callout shows a corrector.

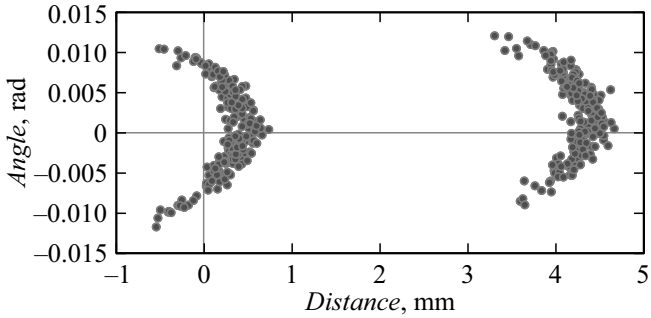

Figure 11. Phase diagrams of beams with masses 100 and 100.1 without a magnetic corrector.

$$S_{12} = \frac{\rho}{\sin\varphi}. \qquad (10)$$

Substituting the calculated values of the angular parameters into these ratios, we obtain the value of the separator's resolution in a linear approximation

$$\tau = \frac{m}{\Delta m} = \frac{S_{z13}}{S_{z12}\overline{z}'} = \frac{S_{z13}\overline{z}}{S_{z12}\eta} = \frac{1.401\overline{z}}{\eta}. \qquad (11)$$

Without the corrector turned on, the second magnet introduces significant nonlinearity, which demonstrates the appearance of phase diagrams of two beams in the focal plane (Figure 11).

But when a potential of 5 V is applied to the first corrector and 45 V to the middle electrode of the second corrector, the linearity is completely restored (Figure 12) and in accordance with Figure 12, b the resolution, determined by the width of the line at half the height, reaches a value of 14 000–15 000.

Since the system is linear, the same resolution value follows from the formula (11) when substituting the width

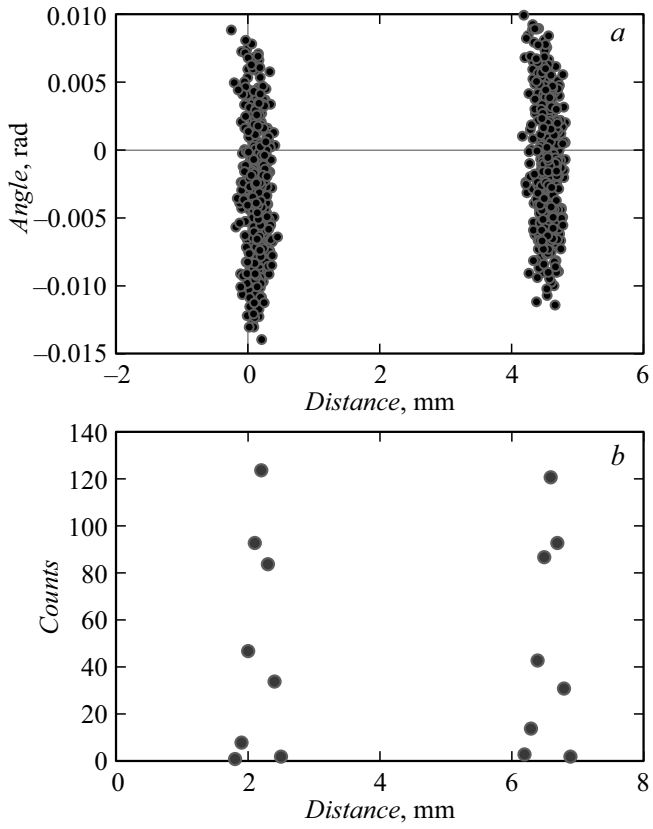

Figure 12. a — phase diagrams of beams with masses $A = 100$ and 100.1; b — lines of the same masses in the focal plane of the magnet with the corrector turned on.

of the angular distribution at half the height from Figure 7, *b*. Thus, these results are completely consistent.

Let's compare the properties of this separator with the properties of the high-resolution separator (HRS) at CERN. This separator based on two magnets that rotate particles in opposite directions is implemented on the ISOLDE 4 [7] installation, where the first magnet rotates ions by 90°, and the second — by 60°. The separator has a complex focusing system consisting of nine quadrupole lenses, two octupole and one sextupole correctors. Moreover, additional multipole correctors are installed on the input faces of both magnets, and the input and output faces of the poles of the second magnet are slightly curved to compensate for second-order aberrations. At the same time, the resolution of this separator is low and is in the range of 3000− 4500, which indicates an obvious nonlinearity of the system.

Conclusion

In this paper, it is shown that optimization based on the requirement of linearity of the system and the use of consequences from Liouville's theorem gives good results. It is also shown that the results obtained for the considered separators in the linear approximation are fully consistent with the simulation results.

In conclusion, we will make a few remarks on the type of phase diagrams for electrostatic focusing and the emittance value of the beam obtained with a surface ionization source. For linearly focused beams, the phase diagrams at the crossover points have the form of parallelograms, as shown in Figure 2, 6, 7, 9 and 10, *a*. Nonlinear diagrams are presented in Figures 3, 4, *a* and 11.

The type of these diagrams cannot be described using an ellipse with Twiss parameters, although this representation is often used in many works on mass-separators. For example, in the study [8], the results of measuring the emittance of a beam with an energy of 30 keV for a separator with a source with surface ionization and axial lenses are given. The measuring device was placed behind the focal plane of the magnet with the angle of rotation of the ions 54.7°. As a result of measurements, the $\pi \cdot (10-20)\,\mathrm{mm} \cdot \mathrm{mrad}$ interval is determined for the emittance. The numbers in parentheses are the product of the lengths of the semi-axes of the ellipse. The same interval is used in the analysis of [7]. Most likely, these limits are overestimated by an order of magnitude. If we take the average value of the interval, then the emittance will be equal to $\pi \cdot 15 = 45\,\mathrm{mm} \cdot \mathrm{mrad}$. Then to obtain a resolution of 14,000 in accordance with the linear formula (12), the width of the linearly focused beam should be equal to 450 and 500 mm in accordance with the formula (5) for the separator shown in Figure 5. These are unrealistically large values, significantly exceeding the aperture of the lenses used.

To increase the resolution of the separators considered, it is necessary to design a new linearly focusing lens with increased dimensions, which will allow a wider beam to be obtained at the same emittance.

Funding

The study was performed in the Petersburg Nuclear Physics Institute as part of an official assignment.

Conflict of interest

The author declares that he has no conflict of interest.

References

[1] V.V. Lukashevich. ZhTF, **90** (3), 471 (2020). (in Russian) DOI: 10.21883/JTF.2020.03.48934.90-19
[2] V.V. Lukashevich. ZhTF, **90** (6), 1016 (2020). (in Russian) DOI: 10.21883/JTF.2020.06.49292.288-19
[3] M. Siladi. *Elektronnaya i ionnaya optika* (Mir, M., 1990). (in Russian)
[4] H. Ewald, H. Hintenberger. *Methoden und Anwendungen der Massenspectroskopie* (Verlag Chemie, Weinheim, 1953)
[5] G. Rudstam. Nucl. Instr. Meth., **139**, 239 (1976).
[6] E. Kugler. Hyperfine Interactions, **129**, 23 (2000).
[7] T.J. Giles, R. Gatherall, V. Fedoseev, U. Georg, E. Kugler, J. Lettry, M. Lindroos. Nucl. Instr. Meth. B, **204**, 497 (2003); CERN/PS 2002-057(OP).
[8] F. Wenander, J. Lettry, M. Lindroos. CERN/PS 2002-045(PP).